JOURNAL OF MATERIALS SCIENCE 35 (2000) 2493–2497

# Finite element analysis of the effect of fibre shape on stresses in an elastic fibre surrounded by a plastic matrix

K. L. GOH*, K. J. MATHIAS*, R. M. ASPDEN‡, D. W. L. HUKINS*,§
*Department of Bio-Medical Physics & Bio-Engineering, and ‡Department of Orthopaedic Surgery, University of Aberdeen, Foresterhill, Aberdeen AB25 2ZD, UK
E-mail: d.hukins@biomed.abdn.ac.uk

The finite element (FE) method was used to calculate the axial and radial stress distributions as a function of axial distance, $z$, from the centre, and radius, $r$, in an elastic fibre surrounded by a plastic matrix. Plastic deformation of the matrix was considered to exert a uniform interfacial stress, $\tau$, along half the length of the fibre. Axisymmetric models were created for uniform cylindrical, ellipsoidal, paraboloidal and conical fibres characterised by an axial ratio, $q$, and half length, $L$. Young's modulus for the material of the fibre and $L$ were arbitrarily assigned values of unity, since they act as scaling factors; $q$ also acts as a scaling factor but was assigned a value of 10 to create models with a fibrous appearance. For the cylindrical fibre, the axial stress increased linearly from the end towards the centre; the radial stress was more evenly distributed. At the other extreme, the conical fibre showed a uniform distribution of axial and radial stress. Results for ellipsoidal and paraboloidal fibres were intermediate between these two extremes. In general, the effect of taper is to lower peak stress at the fibre centre and make the stress distribution throughout the fibre more even. These results are in good agreement with recent analytical theories for the axial distribution of surface radial stress and axial stress along the fibre axis. However, FE models have the advantage of predicting full three-dimensional stress distributions. 

## 1. Introduction

This paper presents the results of a finite element (FE) analysis of the stress distribution in a fibre, which need not be a uniform cylinder, embedded in a plastic matrix. In such a fibre composite system, deformation of the matrix generates an interfacial shear stress, $\tau$. For an elastic matrix $\tau$ is not constant [1]. However, for a plastic matrix the magnitude of $\tau$ is constant along the length of a fibre [2]. The plastic case is important for two reasons. Firstly, it corresponds to the behaviour of the matrix during failure. Secondly, a constant magnitude for $\tau$ corresponds to the physically reasonable case of a constant number of interactions per unit area between fibre and matrix [3, 4]. There are well-established analytical models which show that $\tau$ generates an axial tensile stress, but no compressive stress, in a uniform cylindrical fibre [1, 5]. However, it has been found that the fibres which reinforce some biological composites are tapered [6–8].

Recently, a theory has been developed for the stress distribution in tapered fibres embedded in a plastic matrix [4]. The fibres were modelled as a cone, a paraboloid and an ellipsoid with an axial ratio $q$ (see Section 2.1 for further details). The theory predicts that there will be a radial compressive stress, $\sigma_r$, as well as an axial tensile stress, $\sigma_z$, in these tapered fibres given by

$$\sigma_r = -(\tau/q)\, f_r(Z) \text{ and } \sigma_z = \tau q\, f_z(Z) \qquad (1)$$

where the form of $f_r(Z)$ and $f_z(Z)$ depend on the fibre shape and are both unity for a cone. Here $Z$ represents a fractional distance between the centre of a fibre and its end (see Section 2.2 for further details). Thus $\tau/q$ acts as a scaling factor for the radial stress and $\tau q$ acts as a scaling factor for the axial stress [4]. Strictly, $\sigma_r$ is the radial stress at the surface of the fibre and $\sigma_z$ is the axial stress along the fibre axis. The FE model was developed for two reasons. Firstly, it was developed to check the predictions of the theory. The second reason was to investigate the radial distribution of the radial and axial stresses. These distributions need not be constant and cannot be predicted by the analytical approach. In this paper the FE model is used to investigate stress distributions in a uniform cylinder, a cone, a paraboloid and an ellipsoid when subjected to an interfacial stress of constant magnitude.

§ Author to whom all correspondence should be addressed.

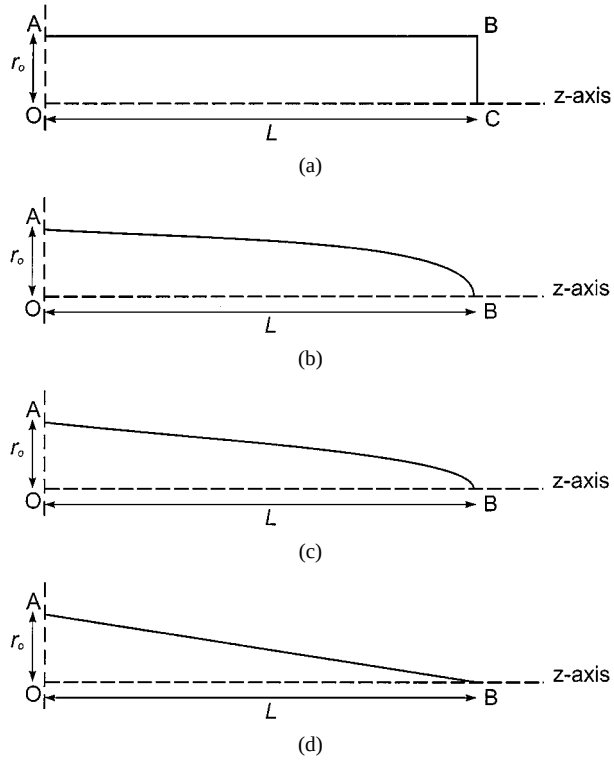


*Figure 1* Models for (a) uniform cylindrical, (b) ellipsoidal, (c) paraboloidal and (d) conical fibres. Each model is developed from a curve in the upper right-hand quadrant which is reflected and rotated (see Section 2.1) to generate an axisymmetric fibre (see Section 2.5). For each shape the radius, $r_o$, at the centre of the fibre and the half length, $L$, of a fibre are marked.

## 2. Methods

### 2.1. Fibre models

Fig. 1 shows upper right-hand quadrants of plane sections through fibres with the following shapes: a uniform cylinder, an ellipsoid, a paraboloid and a cone. A cylindrical polar coordinate system ($r$, $\phi$, $z$) was defined to have its origin at the fibre centre, O, where $r$ denotes the radius of the fibre (which may vary along its length), $\phi$ is an azimuthal angle and $z$ lies along the fibre axis. The axial ratio was defined by $q = L/r_o$, where $r_o$ is the radius of the fibre at the origin and $L$ is the half length of the fibre. The complete fibre model can be generated by reflecting about OA (in Fig. 1) and rotating about OC (in Fig. 1a) or OB (in Fig. 1b–d).

For the purposes of the FE analysis, the shape of the fibre surface was defined by the equations which describe the appropriate cross-section for $0 \leq z \leq L$. For a uniform cylinder this is given by

$$r = r_o. \tag{2}$$

An ellipsoidal fibre is defined by

$$r = r_o\sqrt{1 - \left(\frac{z}{L}\right)^2}, \tag{3}$$

a paraboloidal fibre by

$$r = r_o\sqrt{1 - \left(\frac{z}{L}\right)}, \tag{4}$$

and a conical fibre by

$$r = r_o\left[1 - \left(\frac{z}{L}\right)\right]. \tag{5}$$

Equations 2–5 were used to generate the coordinates that described the profiles of the two-dimensional models for each of the four fibres. Axisymmetric computer models were created from these coordinates using ANSYS (version 5.4; ANSYS, Inc., Houston, PA).

### 2.2. Fibre properties

The Young's modulus of the fibre material was assigned a value of unity since it acts as a scaling factor. Poisson's ratio was assigned a single value (0.3) since this paper is concerned solely with determining stresses which are independent of its value (unlike strains). Since $q$ acts as a scaling factor (see Section 1), it was assigned a value of 10 which yields models with a fibrous appearance (Fig. 1) but avoids difficulties in meshing models with large values of $q$. Since $Z = z/L$, in Section 1, it also follows that $L$ acts as a scaling factor when stress is plotted as a function of $z$; therefore, it was assigned a value of unity.

### 2.3. Meshing and optimisation

Each model was initially meshed using the default mesh generator in ANSYS. Element shape and element size [9] were varied to produce stress distributions which were smooth curves and optimised the level of agreement with the analytical models. Six-node triangular elements were found to be better, according to these criteria, than eight-node quadrilateral elements. The number of elements used for each shape ranged from approximately 13000 (cone) to 15000 (cylinder). The computational time was not affected appreciably by the number of elements. Therefore, the maximum number of elements allowed by ANSYS was used.

### 2.4. Boundary conditions

To ensure that the model had the symmetry described in Section 2.1, the nodes lying along OA, in Fig. 1, were constrained to prevent any displacement in the $z$-direction.

The constant shear stress, $\tau$, tangential to the surface of the fibre was assigned a value of unity as it acts as a scaling factor (see Section 1). This interfacial stress gives rise to an interfacial force. The interfacial force, $F_i$, acting on the $i$th node, along AB, is given by

$$F_i = \tau\pi l_i(r_i + r_{i+1}) \tag{6}$$

where $l_i$ is the distance between the $i$th and $(i+1)$th nodes; $r_i$ and $r_{i+1}$ are the radii of these nodes and, hence, of the toroidal surface element. Equation 6 relates $\tau$ to $F_i$ by multiplying it by the outer surface area of this element which is the surface of the frustum of a cone. For input into the FE model, each value of $F_i$ was resolved into components parallel with and perpendicular to the $z$-axis of the cylindrical polar coordinate system (Section 2.1).

### 2.5. Solving and postprocessing

The FE models were solved for the stresses using the default solver provided by ANSYS. Equation 1 shows that $\tau/q$ acts as a multiplier for the radial stress, $\sigma_r$. Since $\tau$ and $q$ were assigned arbitrary values, $\sigma_r q/\tau$ was plotted as a function of $z$ and $r$ using Matlab (version 5.0; The MathWorks, Inc., Massachusetts, USA). Similarly, Equation 1 shows that $\tau q$ acts as a multiplier for the axial stress, $\sigma_z$. Since $\tau$ and $q$ were assigned arbitrary values, $\sigma_z/\tau q$ was plotted as a function of $z$ and $r$. These plots enable values of $\sigma_r$ and $\sigma_z$ to be calculated for a fibre with a known value of $q$ when subjected to a known value of $\tau$.

## 3. Results

The axial stress distributions for the different shapes of fibre are shown in Fig. 2. For the uniform cylindrical fibre, the stress rose linearly, in the axial direction, from zero at its end to a maximum value; $\sigma_z/\tau q$ had its greatest value of 2 at the centre of the fibre (Fig. 2a). For the ellipsoidal (Fig. 2b) and paraboloidal (Fig. 2c) fibres, the stresses also increased from zero at the end but were distributed more evenly than for the uniform cylinder. In the ellipsoidal fibre, $\sigma_z/\tau q$ reached a maximum value of about 1.5 at the centre; in the paraboloidal fibre it reached a value of about 1.3. The stress was constant along the whole length of the conical fibre with $\sigma_z/\tau q = 1$ (Fig. 2d). Note that the uniform cylinder, ellipsoid, paraboloid and cone are progressively more tapered in shape. Tapering the fibre has the effect of lowering the peak stress at its centre and making the distribution more uniform over its length. Variation across the fibre radius for a uniform cylindrical fibre was usually small (less than 0.5%) with the highest values along the fibre axis; an exception occurred at the surface, near the plane of symmetry, but is likely to be an artefact of the modelling procedure. There was no apparent dependence of stress on radius for a conical fibre and, as before, the ellipsoidal and paraboloidal fibres had distributions intermediate between the extremes of the uniform cylinder and the cone.

The radial stress distributions at the fibre surface are defined by the radial component of the applied shear stress, which is compressive; the distribution of radial stress values is shown in Fig. 3 for all four fibre shapes. In practice, $\sigma_r q/\tau$ was plotted, instead of the stress, $\sigma_r$, for the reason discussed in Section 2.5. For the cylindrical fibre, the radial stress is zero across the whole radius over most of the length of the fibre; however, the stress becomes increasingly compressive at the fibre end and there is a region of tensile stress near the fibre centre (Fig. 3a). The conical fibre shows no variation of radial stress (Fig. 3d). There is a constant compressive stress over the whole cross-section of the fibre, corresponding to the radial component of the applied shear stress. Once again the ellipsoidal and paraboloidal fibres show behaviour intermediate to these extremes, with the stress distribution in the less tapered ellipsoidal fibre (Fig. 3b) being similar to that of the cylinder and that of the more tapered paraboloidal fibre showing a distribution closer to that of the cone.

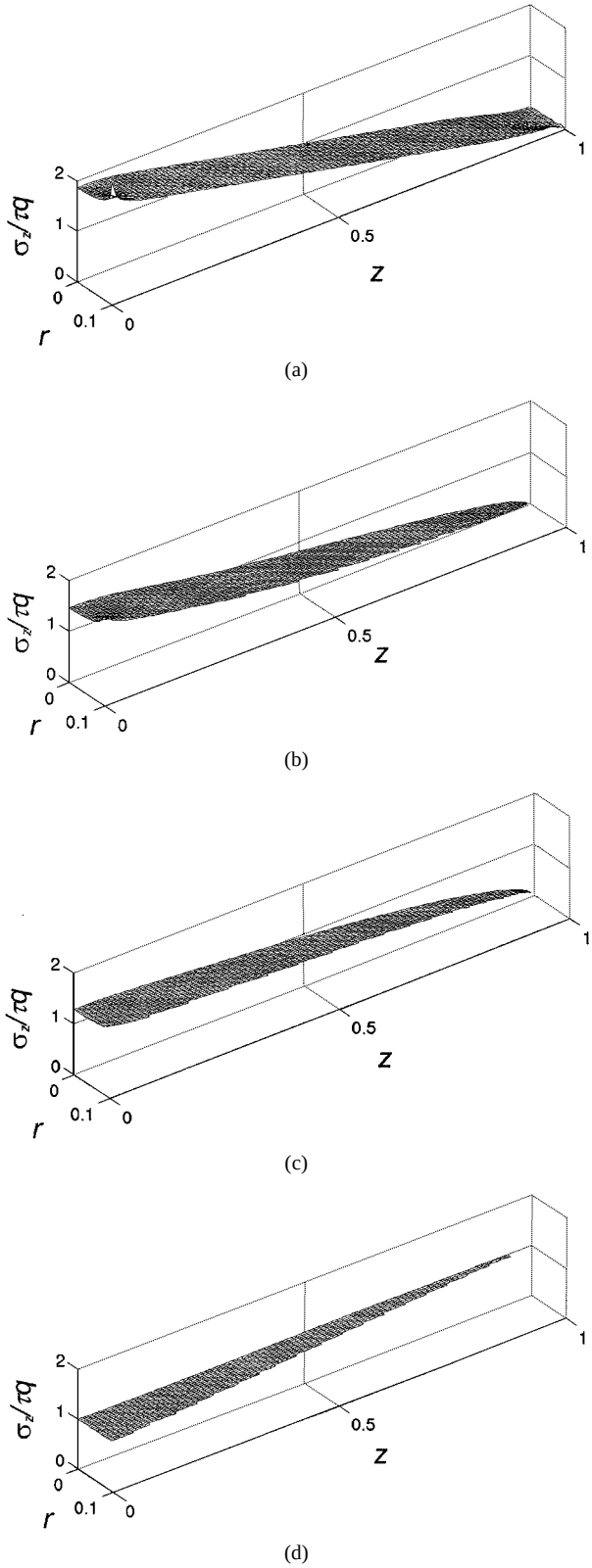


*Figure 2* Distribution of $\sigma_z/\tau q$ plotted against axial displacement, $z$, and radius, $r$, for (a) uniform cylindrical, (b) ellipsoidal, (c) paraboloidal and (d) conical fibres. Here $\sigma_z$ is the axial stress induced in a fibre of axial ratio $q$ (see Section 2.1) as a result of an interfacial stress $\tau$ (see Section 1).

## 4. Discussion

The axial distribution of axial stress, $\sigma_z$, determined from the FE models is in excellent agreement with theoretical predictions. Fig. 4a compares the FE results with the theoretical axial distribution of $\sigma_z/\tau q$ for a

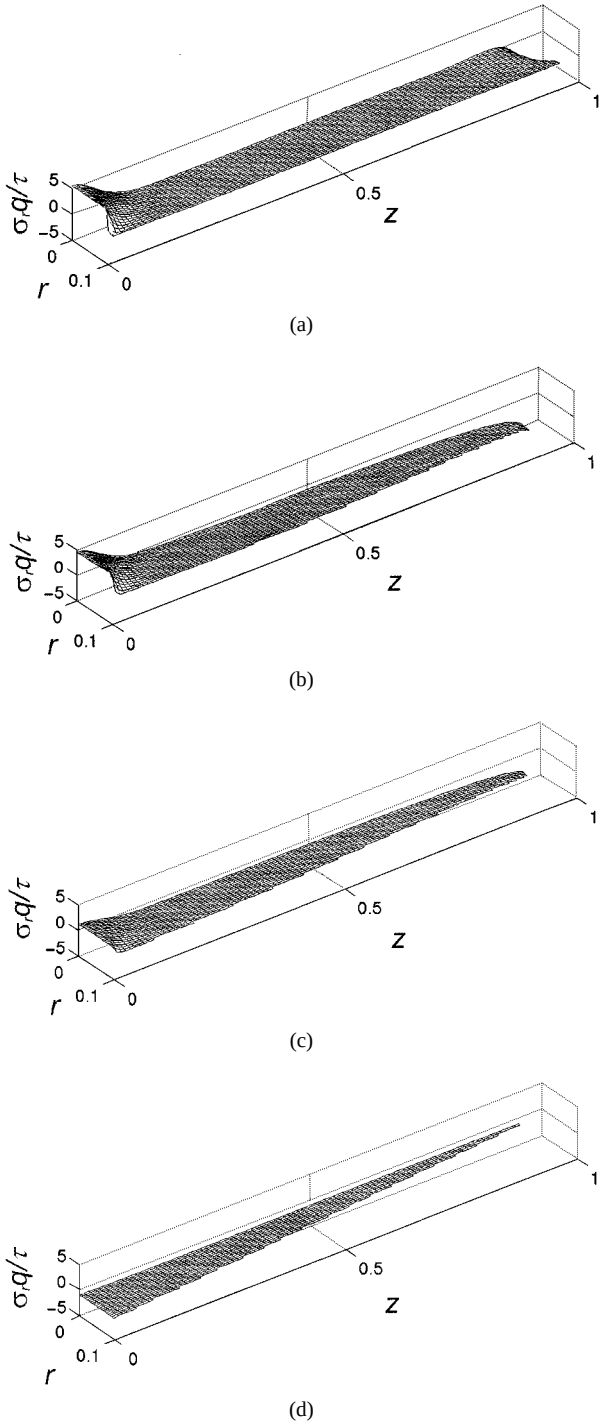


*Figure 3* Distribution of $\sigma_r q/\tau$ plotted against axial displacement, $z$, and radius, $r$, for (a) uniform cylindrical, (b) ellipsoidal, (c) paraboloidal and (d) conical fibres. Here $\sigma_r$ is the radial stress induced in a fibre of axial ratio $q$ (see Section 2.1) as a result of an interfacial stress $\tau$ (see Section 1).

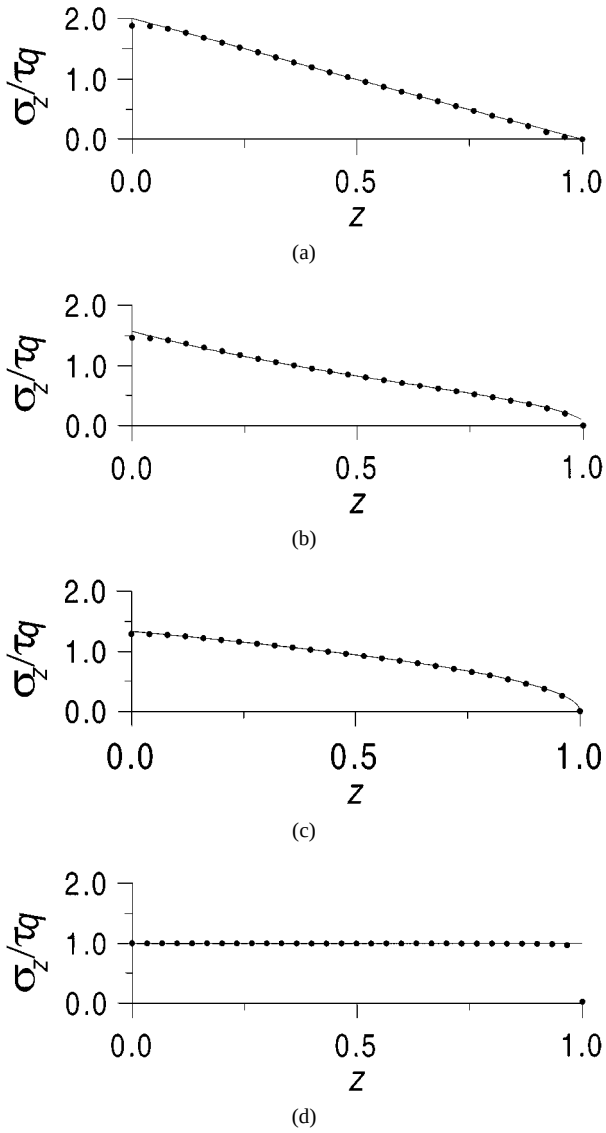


*Figure 4* FE results (filled circles) compared with theoretical results (continuous line) for $\sigma_z/\tau q$ plotted against axial distance, $z$, for (a) uniform cylindrical, (b) ellipsoidal, (c) paraboloidal and (d) conical fibres. Here $\sigma_z$ is the axial stress induced in a fibre of axial ratio $q$ (see Section 2.1) as a result of an interfacial stress $\tau$ (see Section 1). Formulae for calculating theoretical results are published elsewhere [4].

uniform cylinder. The theoretical expression was calculated using the generally accepted theory for a plastic matrix [1, 5] which is a special case of the general theory for fibres of any shape [4]. The result for a uniform cylinder has also been obtained previously [10] by applying Filon's analysis [11]. Similarly good agreement between FE results and the theoretical axial distribution of $\sigma_z/\tau q$ was obtained for ellipsoidal (Fig. 4b), paraboloidal (Fig. 4c) and conical fibres (Fig. 4d). In these cases, the theory for tapered fibres [4] was used to calculate the theoretical stress distributions.

The axial distribution of surface radial stress, $\sigma_r$, determined from the FE models is also in excellent agreement with theoretical predictions (Fig. 5). The same theories were used to calculate the theoretical distributions of radial stress for the uniform cylindrical [1], ellipsoidal, paraboloidal and conical [4] fibres as were used for axial stress.

Thus the FE models agree with the predictions of theory, if $\tau$ is considered to be constant along the length of a fibre. However, FE models have a further application. Current theories are restricted to predicting the axial distribution of radial stress, at the fibre surface only, and of axial stress, along the fibre axis only. In contrast, FE models can provide information on the full three-dimensional stress distribution throughout a fibre. Previously the FE method has been used to investigate the interfacial stress distribution for a uniform cylindrical elastic fibre surrounded by an elastic matrix [12]. Now it has been used to investigate stress distributions

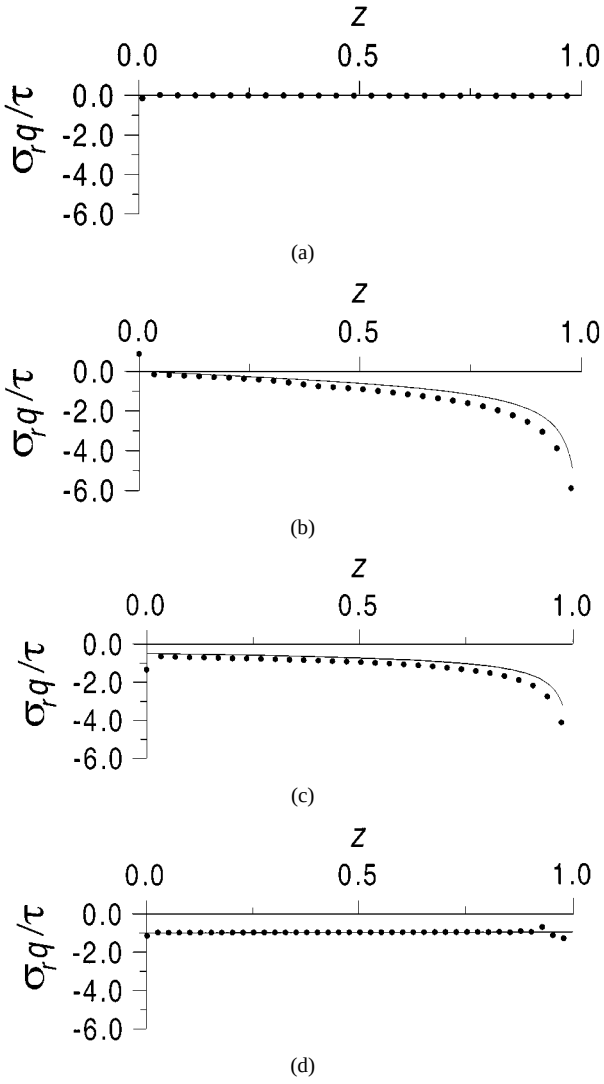


*Figure 5* FE results (filled circles) compared with theoretical results (continuous line) for $\sigma_r q/\tau$ plotted against axial distance, $z$, for (a) uniform cylindrical, (b) ellipsoidal, (c) paraboloidal and (d) conical fibres. Here $\sigma_r$ is the radial stress induced in a fibre of axial ratio $q$ (see Section 2.1) as a result of an interfacial stress $\tau$ (see Section 1). Formulae for calculating theoretical results are published elsewhere [4].

in fibres, which need not be uniform cylinders, when embedded in a plastic matrix.

The FE results enable us to draw two important conclusions on the effect of taper on the stress distribution within an elastic fibre embedded in a plastic matrix. Firstly, comparison of Figs 2 and 3 shows that radial stresses are much less than axial stresses. In order to understand this conclusion note that $\tau$ is a constant and that, for real fibres, $q$ will be very large; thus $\sigma_z$ will be much greater than $\sigma_r$. Secondly, increasing the taper lowers the peak stress at the fibre centre and distributes the axial stress more evenly (see Section 3). In the extreme case of a conical fibre, the axial and radial stresses are both evenly distributed throughout the fibre. Since a cone has only one-third the volume of a uniform cylinder of the same length and radius, conical fibres then represent a more efficient use of a given volume of reinforcing material than uniform cylindrical fibres.


## Acknowledgements

We thank Dr. J. R. Meakin for comments on the paper, the University of Aberdeen for an award of a university postgraduate studentship (to KLG) and the Medical Research Council for an award of a senior fellowship to (RMA).


## References


1. H. L. COX, *Br. J. appl. Phys.* **3** (1952) 72.
2. A. KELLY and W. R. TYSON, *J. Mech. Phys. Solids* **13** (1965) 329.
3. R. M. ASPDEN, *Proc. R. Soc. Lond. B* **258** (1994) 195.
4. K. L. GOH, R. M. ASPDEN, K. J. MATHIAS and D. W. L. HUKINS, *Proc. R. Soc. Lond. A* **455** (1999) 3351.
5. B. D. AGARWAL and L. J. BROUTMAN, "Analysis and Performance of Fibre Composites," (John Wiley & Sons, New York, 1980) p. 73.
6. D. F. HOLMES, J. A. CHAPMAN, D. J. PROCKOP and K. E. KADLER, *Proc. Natl. Acad. Sci.* **89** (1992) 9855.
7. J. A. TROTTER, F. A. THURMOND and T. J. KOOB, *Cell Tissue Res.* **275** (1994) 451.
8. J. E. DEVENTE, G. E. LESTER, J. A. TROTTER and L. E. DAHNERS, *J. Electron Microsc.* **46** (1997) 353.
9. A. M. NIAZY, *BENCHmark* July (1998) 6.
10. R. M. ASPDEN, *J. Mater. Sci.* **29** (1994) 1310.
11. L. N. G. FILON, *Phil. Trans. R. Soc. Lond. A* **198** (1902) 147.
12. A. S. CARRARA and F. J. MCGARRY, *J. Comp. Mat.* **2** (1968) 222.



*Received 17 March*
*and accepted 22 November 1999*